Hindawi
Advances in Condensed Matter Physics
Volume 2023, Article ID 9556764, 14 pages
https://doi.org/10.1155/2023/9556764

Research Article

Theoretical Investigation of the Interplay of Superconductivity and Magnetism in $Ba_{1-x}K_xFe_2As_2$ Superconductor in a Two-Band Model by Using the Bogoliubov Transformation Formalism

Gedefaw Mebratie [1] **and Tigabu Bekele** [2]

[1]*Department of Physics, College of Natural and Computational Sciences, Mekdela Amba University, Tulu Awuliya, Ethiopia*
[2]*Department of Chemistry, College of Natural and Computational Sciences, Mekdela Amba University, Tulu Awuliya, Ethiopia*

Correspondence should be addressed to Tigabu Bekele; tgbekele19@gmail.com

Received 2 December 2022; Revised 1 March 2023; Accepted 28 July 2023; Published 29 August 2023

Academic Editor: Junjie Li

The main focus of this article is to investigate the theoretical interplay of magnetism and superconductivity in a two-band model for the iron-based superconductor $Ba_{1-x}K_xFe_2As_2$. On the basis of experimental results, the two-band model Hamiltonian was considered. We obtained mathematical statements for the superconductor $Ba_{1-x}K_xFe_2As_2$ superconducting (SC) transition temperature, spin-density-wave (SDW), transition temperature, superconductivity order parameter, and SDW order parameter from the Bogoliubov transformation formalism and the model Hamiltonian. Furthermore, an expression for the dependence of the SDW transition temperature on the SDW order parameter and the dependence of the SC transition temperature on the SDW order parameter was obtained for $Ba_{1-x}K_xFe_2As_2$. By substituting the experimental and theoretical values of the parameters in the derived statements, phase diagrams of the SC transition temperature versus the SDW order parameter and the SDW transition temperature versus the SDW order parameters have been plotted to demonstrate the dependence of the SDW order parameter on transition temperatures. By combining the two-phase diagrams, we depicted the possible coexistence of superconductivity and magnetism for the $Ba_{1-x}K_xFe_2As_2$ superconductor. The phase diagrams of temperature versus SC order parameter and temperature versus SDW order parameter were also plotted to show the dependence of order parameters on temperature for the $Ba_{1-x}K_xFe_2As_2$ superconductor.

1. Introduction

Fe-based superconductors (FebSc), which greatly build up the family of unconventional superconductors, have many different systems. The major FebSc systems are 1111, 122, 111, 11, 245, 42622, 1144, and 12442 (e.g., LaFeAsO, $Ba_{1-x}K_xFe_2As_2$, LiFeAs, $FeSe_{1-x}Te_x$, $Rb_2Fe_4Se_5$, $Sr_4V_2O_6Fe_2As_2$, $RbEuFe_4As_4$, and $KCa_2Fe_4As_4F_2$) [1–5]. Iron-based square-planar sheets, which are essential for the unconventional superconductivity of all FebSc systems, represent their shared structural component [6]. The parent compounds of FebSc systems are antiferromagnets, spin-density-wave (SDW) metals, and they are magnetic bad metals. Increasing doping in 122 systems can destroy antiferromagnetism and lead to superconductivity [7]. Superconductivity occurs in specific planes, Fe-As plane [8]. The iron-containing plane of the superconductor, in which pnictogen or chalcogen atoms protrude above and below the plane, is not flat because the pnictogen and chalcogen atoms are much larger than iron atoms [9]. The pnictogen and chalcogen atoms are tightly grouped in a tetrahedral structure [10]. Due to the close packing of the Fe atoms, the five Fe 3d orbitals serve as charge carriers in superconductivity [11]. The sign-changing s-wave symmetry characterizes the FebSc symmetry [12].

Most of the iron-pnictides become superconductors only when doped (added an impurity) with holes or electrons. T_c depends on doping concentration [13]. For the 122 iron-based superconductors family, AFe_2An_2, where (A indicates alkaline earth metals such as Ba, Sr or Ca and Eu) and An is a

pnictide (As, P), superconductivity can be achieved with the introduction of dopants [14]. There are several ways to introduce dopants [15]. These are (1) hole doping is achieved with substituting A for monovalent B^+ (B = Cs, K, Na) atoms partially in the blocking layer, and this substitution should add an excess hole into the system, for example, $Ba_{1-x}K_xFe_2As_2$ [16, 17] (2) partially substitute Fe for transition metals (Co, Ni, Pd, Rh) into FeAs layers and yields electrons into the system. In this method, dopants are directly doped into the Fe layer, which can stabilize the system; for example, Co ($A(Fe_{1-x}Co_x)_2As_2$), Rh ($A(Fe_{2-x}Rh_x)As_2$), Ni ($A(Fe_{1-x}Ni_x)_2As_2$) [18–20] and we get electron-doped pnictides that form an abundant phase diagram where superconductivity and magnetism exist together, and (3) replacing arsenic partially with phosphorus, and phosphorus generates a chemical pressure effect that suppress SDW and emerges superconductivity at the corresponding unit cell volume [21, 22].

The parent compound $BaFe_2As_2$ is an iron arsenide compound and crystallizes with the tetragonal $ThCr_2Si_2$ type structure, space group I4/mmm [23]. Its crystal structure and SDW transition are strongly affected by hole doping with potassium [24]. The compound $BaFe_2As_2$ changes structural and magnetic transitions simultaneously at $T_s = T_N \approx 140\,\mathrm{K}$ [25]. Magnetic transition is strongly coupled with structural distortion. Potassium substitutions with hole doping suppress the SDW state of $BaFe_2As_2$, resulting in the befall of superconductivity [26]. The suppression of long-range magnetic ordering and the emergence of the superconducting (SC) state at the same time are correlated, suggesting that the spin fluctuation of the Fe moments is crucial in creating the superconductive state [27]. The coupling between lattice and spins results from the proximity of the structural and magnetic transitions [28]. The crystal distortion is driven by magnetisms because lower symmetry allows the spins to order and thus relieve magnetic frustrations [6]. Superconductivity, which is closely related to electron pair instability on the Fermi surface, SDW, which has been deduced from the nesting Fermi surface and observed directly in neutron diffraction experiments in the $BaFe_2As_2$ (122) class of materials. The same electronic state would participate in both the SC and SDW electron-pairs instability of the Fermi surface, and indeed the hole and electron-like Fermi sheets in $Ba_{1-x}K_xFe_2As_2$ have been observed [29].

Experiment has been revealed that in potassium substitution barium iron arsenide superconductor ($Ba_{1-x}K_xFe_2As_2$), superconductivity appears for $0.1 \le x \le 1$ in both the orthorhombic and tetragonal phases and for $0.1 \le x < 0.4$, the SDW and SC orders interplay at low temperature [30]. The coexistence of magnetism and superconductivity strongly emphasizes that magnetic spin fluctuations are involved in the Cooper pairing in Fe-based superconductors [24]. As the doping level (x in $Ba_{1-x}K_xFe_2As_2$) increases, the electron Fermi pocket continuously shrinks, whereas the hole pocket becomes larger. SDW ordering coexisting with superconductivity at $= 0.2(T_c = 24\,\mathrm{K})$. When the doping concentration reaches 0.3, the SDW transition is completely suppressed, and T_c increases to 33 K and at $x = 0.4$, $T_c = 38\,\mathrm{K}$. The electron pocket finally vanishes beyond $x = 1$, where superconductivity also disappears. In this article, we study the interaction (coexistence) between magnetism and superconductivity in a two-band model for the iron-based superconductor $Ba_{1-x}K_xFe_2As_2$ by using the Bogoliubov transformation formalism.

Based on the concepts of electronic structure, this article theoretically investigates the coexistence of magnetism and superconductivity with potassium substitution (or hole doping) in the blocking layer of barium iron arsenide ($Ba_{1-x}K_xFe_2As_2$) superconductor in the two-band model. By considering a two-band model of Hamiltonian and using the Bogoliubov transformation formalism methodology, It tried to find the mathematical expression for the SC critical temperature (T_c), SC order parameter (Δ_s), the SDW order parameter (M) and SDW transition temperature (T_M).

2. Mathematical Formulation of the Problem

A system of Hamiltonian conduction electron interacting with phonons for the interplay of superconductivity and magnetism in our compound ($Ba_{1-x}K_xFe_2As_2$) in a two-band model, band a and band b, can be expressed as follows [31–35]:

$$\begin{aligned}\hat{H} = &\sum_{k\sigma}\varepsilon_s(k)\hat{a}^{\dagger}_{k\sigma}\hat{a}_{k\sigma} + \sum_{k\sigma}\varepsilon_b(k)\hat{b}^{\dagger}_{k\sigma}\hat{b}_{k\sigma} + \sum_{k}V^{sc}_{k}\\ &\left(\hat{a}^{\dagger}_{k\uparrow}\hat{a}^{\dagger}_{-k\downarrow}\hat{b}_{k\uparrow}\hat{b}_{-k\downarrow} + \hat{b}^{\dagger}_{k\uparrow}\hat{b}^{\dagger}_{-k\downarrow}\hat{a}_{k\uparrow}\hat{a}_{-k\downarrow}\right)\\ &+\sum_{k\sigma}U^{m}_{k\sigma}\hat{a}^{\dagger}_{k\sigma}\hat{b}_{k\sigma}\hat{b}^{\dagger}_{k\sigma}\hat{a}_{k\sigma}.\end{aligned} \tag{1}$$

Here, the first term is the kinetic energy. The second term is the kinetic energy of holes. The third term is the pair interaction of the SC order parameter, and the fourth term is the pair hopping between the fermion SC channel due to magnetic interactions with some coupling constant ($U^m_{k\sigma}$). k and σ are the wave vector and the spin projection on the z-axis. V_k is the interaction potential of fermions, ε_s and ε_b energies of free electrons measured with respect to the chemical potential. $\hat{a}^{\dagger}_{k\uparrow}\hat{a}_{k\downarrow}$ and $\hat{b}^{\dagger}_{k\uparrow}\hat{b}_{k\downarrow}$ are creation (annihilation) operators of the electrons and holes, respectively.

To decouple the model Hamiltonian, one uses the mean-field approximation, and thus the mean-field Hamiltonian of both SC state and SDW state, expressed as follows:

$$\begin{aligned}\hat{H} = &\sum_{k\sigma}\varepsilon_s(k)\hat{a}^{\dagger}_{k\sigma}\hat{a}_{k\sigma} + \sum_{k\sigma}\varepsilon_b(k)\hat{b}^{\dagger}_{k\sigma}\hat{b}_{k\sigma}\\ &+\sum_{k}\Delta_s(k)\left(\hat{a}^{\dagger}_{k\uparrow}\hat{a}^{\dagger}_{-k\downarrow} + h.c\right) + \sum_{k}\Delta_b(k)\left(\hat{b}^{\dagger}_{k\uparrow}\hat{b}^{\dagger}_{-k\downarrow} + h.c\right)\\ &+\sum_{k\sigma}M\hat{a}^{\dagger}_{\sigma k\uparrow}\hat{b}_{\sigma(k+p)\downarrow} + h.c,\end{aligned} \tag{2}$$

where the mean fields (order parameters) are as follows:

$$\Delta_s = \sum_{k}V^{sc}_{k}\left\langle\hat{b}^{\dagger}_{k\uparrow}, \hat{a}^{\dagger}_{-k\downarrow}\right\rangle, \tag{3}$$

$$\Delta_b = \sum_k V_k^{sc} \left\langle \hat{a}_{k\uparrow}^{\dagger}, \hat{a}_{-k\downarrow}^{\dagger} \right\rangle, \tag{4}$$

where V_k^{sc} is the SC interaction potential.

$$M(k) = \sum_k U_{k\sigma}^{m} \left\langle \hat{a}_{k\uparrow}^{\dagger}, \hat{b}_{(k+p)\downarrow} \right\rangle, \tag{5}$$

where $U_{k\sigma}^{m}$ is the magnetic interaction potential.

2.1. Pure SC State. A Bogoliubov transformation can be used to drive the gap equations by diagonalizing the mean-field Hamiltonian. That means a simple 2D rotation can diagonalize the mean-field Hamiltonian. Such a rotation is equivalent to introducing Bogoliubov operators, where the fermionic anticommutation relations remain valid. This kind of rotation is known as canonical or Bogoliubov transformation. The mean-field Hamiltonian in pure SC state Equation (2) can be written as follows:

$$\begin{aligned}\hat{H} = &\sum_{k\sigma} \varepsilon_s(k) \hat{a}_{k\sigma}^{\dagger} \hat{a}_{k\sigma} + \sum_{k\sigma} \varepsilon_b(k) \hat{b}_{k\sigma}^{\dagger} \hat{b}_{k\sigma} \\ &+ \sum_k \Delta_s(k) \left(\hat{a}_{k\uparrow}^{\dagger} \hat{a}_{-k\downarrow}^{\dagger} + h.c \right) + \sum_k \Delta_b(k) \left(\hat{b}_{k\uparrow}^{\dagger} \hat{b}_{-k\downarrow}^{\dagger} + h.c \right).\end{aligned} \tag{6}$$

The mean-field Hamiltonian in Equation (6) can be diagonalized using the relevant Bogoliubov transformation or quasi-particle transformation, and its diagonalized form is as follows:

$$H_{sc} \approx \sum_{k\sigma} \hat{\phi}_{k\sigma a}^{\dagger} \hat{H}_{ka} \hat{\phi}_{k\sigma a} + \sum_{k\sigma} \hat{\phi}_{k\sigma b}^{\dagger} \hat{H}_{kb} \hat{\phi}_{k\sigma b}, \tag{7}$$

$$H_{sc} = \sum_{k\sigma} \hat{y}_{k\sigma a}^{\dagger} \hat{H}_{ka}^{D} \hat{y}_{k\sigma a} + \sum_{k\sigma} \hat{y}_{k\sigma b}^{\dagger} \hat{H}_{kb}^{D} \hat{y}_{k\sigma b}. \tag{8}$$

For this transformation, the Bogoliubov quasiparticle matrix is defined as follows:

$$\begin{aligned}\hat{y}_{k\sigma a}^{\dagger} &= \begin{pmatrix} \hat{g}_{k\uparrow}^{\dagger} \\ \hat{g}_{-k\downarrow} \end{pmatrix} \\ \hat{y}_{k\sigma b}^{\dagger} &= \begin{pmatrix} \hat{c}_{k}^{\dagger} \\ \hat{c}_{-k} \end{pmatrix}.\end{aligned} \tag{9}$$

Their relation to fermion operators is defined as follows:

$$\begin{aligned}\hat{a}_{\uparrow}^{\dagger} &= u_k \hat{g}_{k\uparrow}^{\dagger} + v_k \hat{g}_{-k\downarrow} \\ \hat{b}_{\uparrow}^{\dagger} &= x_k \hat{c}_{k\uparrow}^{\dagger} + y_k \hat{c}_{-k\downarrow},\end{aligned} \tag{10}$$

where u_k, v_k, x_k, and y_k are coherence factors.

The diagonalized Hamiltonian has the form as follows:

$$\hat{H}_{sc} = \sum_{k\sigma} E_g(k) \hat{g}_{k\sigma}^{\dagger} \hat{g}_{k\sigma} + \sum_{k\sigma} E_b(k) \hat{c}_{k\sigma}^{\dagger} \hat{c}_{k\sigma}. \tag{11}$$

The electron operators $\left\langle \hat{a}_{k\uparrow}^{\dagger}, \hat{a}_{-k\downarrow}^{\dagger} \right\rangle$ and $\left\langle \hat{b}_{k\uparrow}^{\dagger}, \hat{b}_{-k\downarrow}^{\dagger} \right\rangle$ can be expressed in terms of the quasiparticle operators as follows:

$$\begin{aligned}\left\langle \hat{a}_{k\uparrow}^{\dagger}, \hat{a}_{-k\downarrow}^{\dagger} \right\rangle &= \left\langle \left(u_k \hat{g}_{k\uparrow}^{\dagger} + v_k \hat{g}_{-k\downarrow} \right) \left(-v_k \hat{g}_{k\downarrow} + \left(u_k \hat{g}_{k\uparrow}^{\dagger} \right) \right) \right\rangle \\ &\approx u_k v_k \left| \left\langle \hat{g}_{k\uparrow}^{\dagger} \hat{g}_{k\uparrow} \right\rangle - \left\langle \hat{g}_{-k\downarrow}^{\dagger} \hat{g}_{-k\downarrow} \right\rangle \right| \\ &= u_k v_k \left| 1 - 2f\left(E_g(k) \right) \right|,\end{aligned} \tag{12}$$

where f is the Fermi–Dirac statistics, E_g is the Energy at Fermi level.

Applying the properties of Fermi–Dirac statistics, the term $|1 - 2f\left(E_g(k)\right)|$ becomes the following:

$$\left| 1 - 2f\left(E_g(k) \right) \right| \approx \tanh \beta \left(\frac{E_g(k)}{2} \right). \tag{13}$$

The coherence factors u_k and v_k related as follows:

$$u_k . v_k = \frac{\Delta_s(k)}{2E_g(k)}. \tag{14}$$

Inserting Equations (13) and (14) into Equation (12), one can get the following:

$$\left\langle \hat{a}_{k\uparrow}^{\dagger}, \hat{a}_{-k\downarrow}^{\dagger} \right\rangle = \frac{\Delta_s(k)}{2E_g(k)} \tanh \beta \left(\frac{E_g(k)}{2} \right). \tag{15}$$

Substituting Equation (15) into Equation (3), the gap parameter $\Delta_s(k)$ becomes the following:

$$\Delta_s = \sum_k V_k^{sc} \frac{\Delta_s(k)}{2E_g(k)} \tanh \beta \left(\frac{E_g(k)}{2} \right), \tag{16}$$

where $E_g = \sqrt{e_s^2(k) + \Delta_s^2(k)}$. Equation (16) is the SC order parameter in the s band.

Similarly, the b-band mean field value is found as follows:

$$\begin{aligned}\left\langle \hat{b}_{k\uparrow}^{\dagger}, \hat{b}_{-k\downarrow}^{\dagger} \right\rangle &= \left| \left(x_k \hat{c}_{k\uparrow}^{\dagger} + y_k \hat{c}_{-k\downarrow} \right) \left(-y_k c_{k\downarrow} + x \hat{c}_{k\uparrow}^{\dagger} \right) \right| \\ &\approx x_k y_k \left| \left\langle \hat{c}_{k\uparrow}^{\dagger} \hat{c}_{k\uparrow} \right\rangle - \left\langle \hat{c}_{-k\downarrow}^{\dagger} \hat{c}_{-k\downarrow} \right\rangle \right| \\ &= x_k y_k |1 - 2f(E_c(k))|,\end{aligned} \tag{17}$$

where f is the Fermi–Dirac statistics, E_c is the energy at the Fermi level.

Applying the properties of Fermi–Dirac statistics, the term $|1-2f(E_c(k))|$ also becomes the following:

$$|1-2f(E_c(k))| \approx \tanh\beta\left(\frac{E_c(k)}{2}\right). \tag{18}$$

The coherence factors x_k and y_k related as follows:

$$x_k.y_k = \frac{\Delta_b(k)}{2E_c(k)}. \tag{19}$$

Inserting Equations (18) and (19) into Equation (17), one gets the following:

$$\left\langle \hat{b}^{\dagger}_{k\uparrow}, \hat{b}^{\dagger}_{-k\downarrow} \right\rangle = \frac{\Delta_b(k)}{2E_c(k)}\tanh\beta\left(\frac{E_c(k)}{2}\right). \tag{20}$$

Substituting Equation (13) into Equation (4), the gap parameter $\Delta_b(k)$ becomes the following:

$$\Delta_b(k) = \sum_k V_k^{sc}\frac{\Delta_b(k)}{2E_c(k)}\tanh\beta\left(\frac{E_c(k)}{2}\right), \tag{21}$$

where $E_c = \sqrt{\epsilon_b^2(k)+\Delta_b^2(k)}$. Equation (21) is the SC order parameter in the b band.

2.2. Pure SDW State. The Hamiltonian Equation (2) can yield an SDW phase that is a pure magnetic phase for zero SC interaction. The mean-field Hamiltonian for the pure magnetic phase is as follows:

$$\begin{aligned}\hat{H}_m = &\sum_{k\sigma}\varepsilon_s(k)\hat{a}^{\dagger}_{k\sigma}\hat{a}_{k\sigma} + \sum_{k\sigma}\varepsilon_b(k)\hat{b}^{\dagger}_{k\sigma}\hat{b}_{k\sigma}\\ &+\sum_k M\sigma\hat{a}^{\dagger}_{k\uparrow}\hat{b}_{(k+p)\downarrow} + h.c.\end{aligned} \tag{22}$$

The mean-field Hamiltonian in Equation (22) can be diagonalized using the relevant Bogoliubov transformation or quasiparticle transformation, and its diagonalized form is as follows:

$$H_{sc} \approx \sum_{k\sigma}\hat{\phi}^{\dagger}_{mk\sigma}\hat{H}_{mk}\hat{\phi}_{mk\sigma} = \sum_{k\sigma}\hat{y}^{\dagger}_{mk\sigma}\hat{H}^{D}_{mk}\hat{y}_{mk\sigma}. \tag{23}$$

The Bogoliubov quasi-particle matrix for our transformation is as follows:

$$\hat{y}^{\dagger}_{mk\sigma} = \left(\hat{h}^{\dagger}_{mk}\hat{e}^{\dagger}_{mk}\right). \tag{24}$$

Operators in the Hamiltonian are expressed as follows:

$$\begin{aligned}\hat{a}^{\dagger}_{mk} &= t_k\hat{h}^{\dagger}_{k\sigma} + l_k\hat{e}^{\dagger}_{k\sigma}\\ \hat{b}^{\dagger}_{(k+q)\sigma} &= \sigma\left(l_k\hat{h}^{\dagger}_{k\sigma} - t_k\hat{e}^{\dagger}_{k\sigma}\right).\end{aligned} \tag{25}$$

The coherency factors are given by the following:

$$\begin{aligned}t_k.l_k &= \frac{M(k)}{2E(k)}\\ t_k^2.l_k^2 &= \frac{1}{2}\left(1\pm\frac{\varepsilon_s(k)-\varepsilon_b(k)}{E_h(k)-E_e(k)}\right).\end{aligned} \tag{26}$$

Therefore, the diagonalized Hamiltonian will have the form as follows:

$$\hat{H}_{sc} = \sum_{k\sigma}E_h(k)\hat{h}^{\dagger}_{k\sigma}\hat{h}_{k\sigma} + \sum_{k\sigma}E_e(k)\hat{e}^{\dagger}_{k\sigma}\hat{e}_{k\sigma}, \tag{27}$$

where E_h and E_e are the eigenvalues and given by an expression

$E_h = \frac{1}{2}[\varepsilon_s(k)+\varepsilon_b(k)\pm\sqrt{\varepsilon_s(k)-+_b(k)+4M^2}]$ and $E_e = \frac{1}{2}[\varepsilon_s(k)+\varepsilon_b(k)\pm\sqrt{\varepsilon_s(k)-\varepsilon_b(k)+4M^2}]$

Using the Bogoliubov transformation, we defined the SDW state in Equation (23); we can now calculate the expectation value of the operators in Equation (22) to find the SDW gap equation.

$$\begin{aligned}\left\langle \hat{a}^{\dagger}_{k\sigma}\hat{b}_{(k+p)\sigma}\right\rangle &= \left\langle\left(t_k\hat{h}^{\dagger}_{k\sigma} + l_k\hat{e}^{\dagger}_{k\sigma}\right)\sigma\left(l_k\hat{h}_{k\sigma} - t_k\hat{e}_{k\sigma}\right)\right\rangle\\ &= t_kl_k\left(\left\langle\hat{h}^{\dagger}_{k\sigma}\hat{h}_{k\sigma}\right\rangle - \left\langle\hat{e}^{\dagger}_{k\sigma}\hat{e}_{k\sigma}\right\rangle\right)\\ &\approx t_kl_k[f(E_h(k)-f(E_e(k))]\\ &= \frac{M}{2E(k)}\left[\tanh\beta\left[\frac{E_h(k)}{2}\right] - \tanh\beta\left[\frac{E_e(k)}{2}\right]\right].\end{aligned} \tag{28}$$

Substituting Equation (28) into Equation (5), it gives the SDW gap equation.

$$M = \sum_k U\frac{M}{2E(k)}\left[\tanh\beta\left[\frac{E_h(k)}{2}\right] - \tanh\beta\left[\frac{E_e(k)}{2}\right]\right]. \tag{29}$$

2.3. SC Order Parameter (Δ_s). There is clear information that show the coexistence of SDWs and superconductivity in both hole- and electron-doped families in most FebSc [22]. In our compound, $Ba_{1-x}K_xFe_2As_2$, Superconductivity can be obtained by (1) chemical doping [36–38] and/or (2) the application of pressure [39]. The addition of a chemical dopant and/or the application of pressure on $BaFe_2As_2$ results in the eradication of the SDW and, therefore, in the reduction of magnetic order.

Superconductivity is observed when the magnetic order is sufficiently weak; thus, superconductivity and weak magnetic order can still coexist [37, 38, 40]. The exact mechanism for the emergence of superconductivity is, however, still unknown. Therefore, we need to study the coupled system below the SC transition temperature. The mean-field Hamiltonian without the interaction part for both the SC state and the magnetic state is stated in Equation (2). Applying the second quasi-particle transformation to Equation (2), it gives the following:

$$\begin{aligned}\hat{H} = &\sum_{k\sigma} E_g(k)\hat{g}^{\dagger}_{k\sigma}\hat{g}_{k\sigma} + \sum_{k\sigma} E_h(k)\hat{h}^{\dagger}_{k\sigma}\hat{h}_{k\sigma} \\ &+ \sum_k \Delta_s\left(\hat{g}^{\dagger}_{k\uparrow}\hat{g}^{\dagger}_{-k\downarrow} + h.c\right) \\ &+ \sum_k \Delta_b\left(\hat{h}^{\dagger}_{k\uparrow}\hat{h}^{\dagger}_{-k\downarrow} + h.c\right).\end{aligned} \tag{30}$$

Using Nambu notion

$$\hat{H} = \sum_{k\sigma} \hat{\phi}^{\dagger}_{gk\sigma}\hat{H}_{gk}\hat{\phi}_{gk\sigma} + \sum_{k\sigma} \hat{\phi}^{\dagger}_{hk\sigma}\hat{H}_{hk}\hat{\phi}_{hk\sigma}, \tag{31}$$

where the Nambu spinors are as follows:

$$\begin{aligned}\hat{\phi}^{\dagger}_{gk} &= \left(\hat{g}^{\dagger}_{k\uparrow}\hat{g}_{-k\downarrow}\right) \\ \hat{\phi}^{\dagger}_{hk} &= \left(\hat{h}^{\dagger}_{k\uparrow}\hat{h}_{-k\downarrow}\right).\end{aligned} \tag{32}$$

The energy matrix

$$\begin{aligned}\hat{H}_{gk} &= \begin{pmatrix} E_g(k)\Delta_a(k) \\ \Delta_s(k) - E_g(k)\end{pmatrix} \\ \hat{H}_{hk} &= \begin{pmatrix} E_h(k)\Delta_b(k) \\ \Delta_b(k) - E_h(k)\end{pmatrix}.\end{aligned} \tag{33}$$

Diagonalizing Equation (31) for each band gives the following:

$$\hat{H} = \sum_{k\sigma} \hat{y}^{\dagger}_{gk\sigma}\hat{H}^{D}_{gk}\hat{y}_{gk\sigma} + \sum_{k\sigma} \hat{y}^{\dagger}_{hk\sigma}\hat{H}^{D}_{hk}\hat{y}_{hk\sigma}, \tag{34}$$

where $\hat{y}^{\dagger}_{gk}$ and $\hat{y}^{\dagger}_{hk}$ are the Bogoliubov quasi-particle matrix which is defined as the following transformations:

$$\begin{aligned}\hat{y}^{\dagger}_{ka} &= \begin{pmatrix} \hat{A}^{\dagger}_{k\uparrow} \\ \hat{A}_{-k\downarrow}\end{pmatrix} \\ \hat{y}^{\dagger}_{kb} &= \begin{pmatrix} \hat{B}^{\dagger}_{k} \\ \hat{B}_{-k}\end{pmatrix}.\end{aligned} \tag{35}$$

Their relation to fermion operators is defined as follows:

$$\begin{aligned}\hat{g}^{\dagger}_{\uparrow} &= U_k\hat{A}^{\dagger}_{k\uparrow} + V_k\hat{A}_{-k\downarrow} \\ \hat{h}^{\dagger}_{\uparrow} &= X\hat{B}^{\dagger}_{k\uparrow} + Y_k\hat{B}_{-k\downarrow},\end{aligned} \tag{36}$$

where U_k, V_k, X_k and Y_k are coherence factors that satisfy the following relation:

$$\begin{aligned}U_k.V_k &= -\frac{\Delta_s(k)}{2E_g(k)} \\ U_k^2.V_k^2 &= \frac{1}{2}\left(1 \pm \frac{E_g(k)}{\sqrt{E_g^2(k) - \Delta_s^2(k)}}\right),\end{aligned} \tag{37}$$

and

$$\begin{aligned}X_k.Y_k &= -\frac{\Delta_b(k)}{2E_B(k)} \\ X_k^2.Y_k^2 &= \frac{1}{2}\left(1 \pm \frac{E_h(k)}{\sqrt{E_h^2(k) - \Delta_b^2(k)}}\right),\end{aligned} \tag{38}$$

where E_A and E_B are the eigenvalues or excitations and are given by the following:

Where $E_A(k) = \sqrt{\epsilon_s^2(k) + (\Delta_s + M)^2}$ and $E_B(k) = \sqrt{\epsilon_b^2(k) + (\Delta_b - M)^2}$

Therefore, the diagonalized Hamiltonian will have the form as follows:

$$\hat{H} = \sum_{k\sigma} E_A(k)\hat{A}^{\dagger}_{k\sigma}\hat{A}_{k\sigma} + \sum_{k\sigma} E_B(k)\hat{B}^{\dagger}_{k\sigma}\hat{B}_{k\sigma}. \tag{39}$$

Following the same procedure as for the SC state and the magnetic state, the gap equations for both the magnetic and SC states, the gap equations or order parameters are given by the following:

$$\begin{aligned}\Delta_s = &\sum_k V_k^{sc}\frac{\Delta_s(k) + M(k)}{4E_A(k)}\tanh\beta\left(\frac{E_A(k)}{2}\right) \\ &+ \sum_k V_k^{sc}\frac{\Delta_s(k) - M(k)}{4E_A(k)}\tanh\beta\left(\frac{E_B(k)}{2}\right) \\ \Delta_b = &\sum_k V_k^{sc}\frac{\Delta_b(k) + M(k)}{4E_B(k)}\tanh\beta\left(\frac{E_B(k)}{2}\right) \\ &+ \sum_k V_k^{sc}\frac{\Delta_b(k) - M(k)}{4E_B(k)}\tanh\beta\left(\frac{E_A(k)}{2}\right),\end{aligned} \tag{40}$$

where $E_A(k) = \sqrt{\epsilon_s^2(k) + (\Delta_s + M)^2}$ and $E_B(k) = \sqrt{\epsilon_b^2(k) + (\Delta_b - M)^2}$.

Near the edge of the Fermi-surface, there is homogeneity, and the two order parameters can be taken as equal and opposite; with this assumption, we can take $\Delta_b(k) = \Delta_s(k)$,

and $\epsilon_s = \epsilon_b$. With this in mind, the two SC gap equations of Equation (40) are simplified to the following:

$$\Delta_s = \sum_k V_k^{sc} \frac{\Delta_s(k) + M(k)}{4E_A(k)} \tanh \beta \left(\frac{E_A(k)}{2} \right) + \sum_k V_k^{sc} \frac{\Delta_s(k) - M(k)}{4E_B(k)} \tanh \beta \left(\frac{E_B(k)}{2} \right), \tag{41}$$

where $E_A(k) = \sqrt{\epsilon_s^2(k) + (\Delta_s(k) + M(k))^2}$ and $E_B(k) = \sqrt{\epsilon_s^2(k) + (\Delta_s(k) - M(k))^2}$

For simplicity, the interaction potential $V_k^{sc} = V$ and Equation (41) is simplified to the following:

$$\Delta_s = \frac{V}{4} \sum_{k,i=1,2} \Delta_i(k) \frac{\tanh \frac{\beta}{2} \sqrt{\epsilon_s^2(k) + \Delta_i{}^2(k)}}{\sqrt{\epsilon_s^2(k) + \Delta_i{}^2(k)}}, \tag{42}$$

where $\Delta_i = \Delta_s - (-1)^i M$ is called the effective order parameter.

Changing summation to integration in the region $-\hbar\omega_F < \epsilon_s(k) < \hbar\omega_F$ and by introducing the density of state at the Fermi level of the interband interaction, $N(0)$ that is as follows:

$$\sum_k \approx \int_{-\hbar\omega_F}^{\hbar\omega_F} N(0) d\epsilon_s(k). \tag{43}$$

The density of state $N(0)$ is equal to $\sqrt{N_s(0)N_b(0)}$ and Equation (42), becomes the following:

$$\Delta_s = \frac{V}{4} \int_{-\hbar\omega_F}^{\hbar\omega_F} \sqrt{N_s(0)N_b(0)} \Delta_i \frac{\tanh \frac{\beta}{2} \sqrt{\epsilon_s^2(k) + \Delta_i{}^2}}{\sqrt{\epsilon_s^2(k) + \Delta_i{}^2}} d\epsilon_s(k), \tag{44}$$

$$\Delta_s = \frac{V\sqrt{N_s(0)N_b(0)}}{4} \int_{-\hbar\omega_F}^{\hbar\omega_F} \Delta_i \frac{\tanh \frac{\beta}{2} \sqrt{\epsilon_s^2(k) + \Delta_i{}^2}}{\sqrt{\epsilon_s^2(k) + \Delta_i{}^2}} d\epsilon_s(k), \tag{45}$$

$$\frac{4}{V\sqrt{N_s(0)N_b(0)}} = \int_{-\hbar\omega_F}^{\hbar\omega_F} \frac{\Delta_i}{\Delta_s} \frac{\tanh \frac{\beta}{2} \sqrt{\epsilon_s^2(k) + \Delta_i{}^2}}{\sqrt{\epsilon_s^2(k) + \Delta_i{}^2}} d\epsilon_s(k), \tag{46}$$

$$\frac{2}{V\sqrt{N_s(0)N_b(0)}} = \int_0^{\hbar\omega_F} \frac{\Delta_i}{\Delta_s} \frac{\tanh \frac{\beta}{2} \sqrt{\epsilon_s^2(k) + \Delta_j{}^2(k)}}{\sqrt{\epsilon_s^2(k) + \Delta_i{}^2}} d\epsilon_s(k), \tag{47}$$

$$\frac{2}{V\sqrt{N_s(0)N_b(0)}} = \int_0^{\hbar\omega_F} \left(\frac{\Delta_s - M}{\Delta_s} \right) \frac{\tanh \frac{\beta}{2} \sqrt{\epsilon_s^2(k) + (\Delta_s - M)^2}}{\sqrt{\epsilon_s^2(k) + (\Delta_s - M)^2}} d\epsilon_s(k) + \int_0^{\hbar\omega_F} \left(\frac{\Delta_s + M}{\Delta_s} \right) \frac{\tanh \frac{\beta}{2} \sqrt{\epsilon_s^2(k) + (\Delta_s - M)^2}}{\sqrt{\epsilon_s^2(k) + (\Delta_s - M)^2}} d\epsilon_s(k), \tag{48}$$

$$\text{Let} \sim \varphi = V\sqrt{N_s(0)N_b(0)}, \tag{49}$$

$$\frac{1}{\varphi} = \int_0^{\hbar\omega_D} \left(1 - \frac{M}{\Delta_s(k)} \right) \frac{\tanh \frac{\beta}{2} (\epsilon_s^2(k) + (\Delta_s - M)^2)^{\frac{1}{2}}}{(\epsilon_s^2(k) + (\Delta_s - M)^2)^{\frac{1}{2}}} d\epsilon_s(k) + \int_0^{\hbar\omega_F} \left(\frac{\Delta_s + M}{\Delta_s} \right) \frac{\tanh \frac{\beta}{2} \sqrt{\epsilon_s^2(k) + (\Delta_s - M)^2}}{\sqrt{\epsilon_s^2(k) + (\Delta_s - M)^2}} d\epsilon_s(k), \tag{50}$$

$$\frac{2}{\varphi} = \int_0^{\hbar\omega_F} \frac{\tanh \frac{\beta}{2} (\epsilon_s^2(k) + (\Delta_s - M)^2)^{\frac{1}{2}}}{(\epsilon_s^2(k) + (\Delta_s - M)^2)^{\frac{1}{2}}} d\epsilon_k - \int_0^{\hbar\omega_F} \frac{M}{\Delta_s(k)} \frac{\tanh \frac{\beta}{2} (\epsilon_s^2(k) + (\Delta_s - M)^2)^{\frac{1}{2}}}{(\epsilon_s^2(k) + (\Delta_s - M)^2)^{\frac{1}{2}}} d\epsilon_s(k) + \int_0^{\hbar\omega_F} \frac{\tanh \frac{\beta}{2} (\epsilon_s^2(k) + (\Delta_s - M)^2)^{\frac{1}{2}}}{(\epsilon_s^2(k) + (\Delta_s - M)^2)^{\frac{1}{2}}} d\epsilon_k + \int_0^{\hbar\omega_F} \frac{M}{\Delta_s} \frac{\tanh \frac{\beta}{2} (\epsilon_s^2(k) + (\Delta_s - M)^2)^{\frac{1}{2}}}{(\epsilon_s^2(k) + (\Delta_s - M)^2)^{\frac{1}{2}}} d\epsilon_s(k), \tag{51}$$

$$\frac{2}{\varphi} = h_1 + h_2, \tag{52}$$

where

$$h_1 = \int_0^{\hbar\omega_F} \frac{\tanh \frac{\beta}{2} (\epsilon_s^2(k) + (\Delta_s - M)^2)^{\frac{1}{2}}}{(\epsilon_s^2(k) + (\Delta_s - M)^2)^{\frac{1}{2}}} d\epsilon_s(k) - \int_0^{\hbar\omega_F} \frac{M}{\Delta_s} \frac{\tanh \frac{\beta}{2} (\epsilon_s^2(k) + (\Delta_s - M)^2)^{\frac{1}{2}}}{(\epsilon_s^2(k) + (\Delta_s - M)^2)^{\frac{1}{2}}} d\epsilon_s(k), \tag{53}$$

$$h_2 = \int_0^{\hbar\omega_F} \frac{\tanh \frac{\beta}{2} (\epsilon_s^2(k) + (\Delta_s - M)^2)^{\frac{1}{2}}}{(\epsilon_s^2(k) + (\Delta_s - M)^2)^{\frac{1}{2}}} d\epsilon_s(k) + \int_0^{\hbar\omega_F} \frac{M}{\Delta_s} \frac{\tanh \frac{\beta}{2} (\epsilon_s^2(k) + (\Delta_s - M)^2)^{\frac{1}{2}}}{(\epsilon_s^2(k) + (\Delta_s - M)^2)^{\frac{1}{2}}} d\epsilon_s(k), \tag{54}$$

$$h_1 = I_1 + I_2. \tag{55}$$

If $T \longrightarrow T_c, \Delta_s(k) \longrightarrow 0$, and evaluating the integrals,

$$I_1 = \int_0^{\hbar\omega_D} \frac{\tanh \frac{\beta}{2}(\epsilon_s^2(k) + M^2)^{\frac{1}{2}}}{(\epsilon_s^2(k) + M^2)^{\frac{1}{2}}} d\epsilon_s(k). \tag{56}$$

Let $\mu = \beta\sqrt{\epsilon_s^2(k) + M^2}$ and $\sum_{-\infty}^{\infty} \frac{1}{((2n+1)\pi)^2+\mu^2} = \frac{\tanh\frac{\gamma}{2}}{2\gamma}$, then Equation (56) written as follows:

$$= \int_0^{\hbar\omega_D} \frac{2\beta \tanh \frac{\mu}{2}}{2\mu} d\epsilon_s(k), \tag{57}$$

$$\begin{aligned} &= 2\beta \int_0^{\hbar\omega_F} \sum_{-\infty}^{\infty} \frac{1}{(2n+1)^2\pi^2 + \mu^2} d\epsilon_s(k) \\ &= \frac{2}{\beta} \int_0^{\hbar\omega_F} \sum_{-\infty}^{\infty} \frac{1}{\omega_n^2 + \epsilon_s^2(k) + M^2} d\epsilon_s(k). \end{aligned} \tag{58}$$

From Laplacian transform with the Matsuber relation result, we can write Equation (58) as follows:

$$\begin{aligned} &\frac{2}{\beta} \int_0^{\hbar\omega_F} \sum_{-\infty}^{\infty} \frac{1}{\omega_n^2 + \epsilon_s^2(k) + M^2} d\epsilon_s(k) \\ &= \frac{2}{\beta} \int_0^{\hbar\omega_F} \sum_{-\infty}^{\infty} \frac{1}{\omega_n^2 + \epsilon_s^2(k)} d\epsilon_s(k) \\ &\quad -M^2 \frac{2}{\beta} \int_0^{\hbar\omega_F} \sum_{-\infty}^{\infty} \frac{1}{\omega_n^2 + \epsilon_s^2(k)} d\epsilon_s(k), \end{aligned} \tag{59}$$

$$\begin{aligned} &= 2\beta \int_0^{\hbar\omega_F} \sum_{-\infty}^{\infty} \frac{1}{(2n+1)^2\pi^2 + (\beta \in_s(k))^2} d\epsilon_s(k) \\ &\quad -M^2 \int_0^{\hbar\omega_F} \frac{2}{\beta} \sum_{-\infty}^{\infty} \frac{1}{(2n+1)^2 \left(\frac{\pi}{\beta}\right)^2 + \epsilon_s^2(k)} d\epsilon_s(k) \\ &= \int_0^{\hbar\omega_F} \frac{\tanh \beta \frac{\epsilon_s(k)}{2}}{\epsilon_s(k)} d\epsilon_s(k) \\ &\quad -2M^2 \int_0^{\hbar\omega_F} \frac{2}{\beta} \sum_{0}^{\infty} \frac{1}{(2n+1)^2 \left(\frac{\pi}{\beta}\right)^2 + \epsilon_s^2(k)} d\epsilon_s(k). \end{aligned} \tag{60}$$

Apply the following equality.

$$\sum_0^{\infty} \frac{1}{(f^2 + \epsilon_s^2(k))^2} d\epsilon_s(k) = 2\sum_0^{\infty} \frac{1}{f^4(1+z^2)^2} d\epsilon_s(k), \tag{61}$$

where $f^2 = (2n+1)^2 \left(\frac{\pi}{\beta}\right)^2$ and $z^2 = \frac{\epsilon_s^2(k)}{f^2}$

$$I_1 = \int_0^{\hbar\omega_F} \frac{\tanh \beta \frac{\epsilon_s(k)}{2}}{\epsilon_s(k)} d\epsilon_s(k) - \int_0^{\hbar\omega_F} \frac{4}{\beta} \sum_0^{\infty} \frac{M^2}{f^4(1+z^2)^2} d\epsilon_s(k). \tag{62}$$

From the above equality relations $z = \beta \frac{\epsilon_s(k)}{2}$ and $dz = \beta \frac{d\epsilon_s(k)}{2}$

$$I_1 = \int_0^{\frac{\beta}{2}\hbar\omega_F} \frac{\tanh z}{z} dz - \int_0^{\infty} \frac{4}{\beta} \sum_0^{\infty} \frac{M^2}{f^3(1+z^2)^2} dz, \tag{63}$$

$$\begin{aligned} &= \ln\left(\frac{\beta}{2}\hbar\omega_F\right) \tanh\left(\frac{\beta}{2}\hbar\omega_F\right) - \int_0^{\frac{\beta}{2}\hbar\omega_F} \frac{\ln z}{\cosh^2 z} dz \\ &\quad -\frac{4}{\beta} M^2 \sum_0^{\infty} \frac{1}{f^3} \int_0^{\infty} \frac{1}{(1+z^2)^2} dz, \end{aligned} \tag{64}$$

$$\begin{aligned} &= \ln\left(\frac{\beta}{2}\hbar\omega_F\right) \tanh\left(\frac{\beta}{2}\hbar\omega_F\right) - \ln\left(\frac{\pi}{4\gamma}\right) \\ &\quad -\frac{4\beta^2 M^2}{\pi^3} \sum_0^{\infty} \frac{1}{(2n+1)^3} \int_0^{\infty} \frac{1}{(1+z^2)^2} dz, \end{aligned} \tag{65}$$

$$= \ln\left(\frac{\beta}{2}\hbar\omega_F\right) \tanh\left(\frac{\beta}{2}\hbar\omega_F\right) - \ln\left(\frac{\pi}{4\gamma}\right) - \frac{4\beta^2 M^2}{\pi^3} \frac{7}{8} \xi(3) \frac{\pi}{4}. \tag{66}$$

For low-temperature $\tanh\left(\frac{\beta}{2}\hbar\omega_F\right) \longrightarrow 1$ and γ denotes the Euler's constant and its value is given by $\gamma = 1.78$. $\int_0^{\infty} \frac{1}{1+z^2} dz = \frac{\pi}{4}$ and $\sum_0^{\infty} \frac{1}{(2n+1)^p} = (1 - 2^{-p})\xi(p)$ this means $\xi(3) = 1.202$.so after some steps Equation (66) can be written as follows:

$$I_1 = \ln\left(1.14 \frac{\hbar\omega_F}{k_B T_c}\right) - 1.052 \left(\frac{M}{\pi k_B T_c}\right)^2. \tag{67}$$

The second integral I_2 can be calculated using L'Hopitals Rule as follows:

$$I_2 = -\int_0^{\hbar\omega_F} \frac{M}{\Delta_s(k)} \frac{\tanh \frac{\beta}{2}(\epsilon_s^2(k) + (\Delta_s(k) - M)^2)^{\frac{1}{2}}}{(\epsilon_s^2(k) + (\Delta_s(k) - M)^2)^{\frac{1}{2}}} d\epsilon_s(k), \tag{68}$$

$$\begin{aligned} &= -\int_0^{\hbar\omega_F} \lim_{\Delta_{SC}^s \longrightarrow 0} \frac{d}{d\Delta_s(k)} \\ &\quad \left(\frac{M}{\Delta_s(k)} \frac{\tanh \frac{\beta}{2}(\epsilon_s^2(k) + (\Delta_s(k) - M)^2)^{\frac{1}{2}}}{(\epsilon_s^2(k) + (\Delta_s(k) - M)^2)^{\frac{1}{2}}}\right) d\epsilon_s(k), \end{aligned} \tag{69}$$

$$\begin{aligned} &= -\int_0^{\hbar\omega_F} \lim_{\Delta_s(k) \longrightarrow 0} \\ &\quad \left(\frac{M \operatorname{sech}^2 \frac{\beta}{2}(\epsilon_s^2(k) + (\Delta_s(k) - M)^2)^{\frac{1}{2}} \frac{\beta}{2} \frac{\{\Delta_s(k) - M\}}{(\epsilon_s^2(k) + (\Delta_s(k) - M)^2)^{\frac{1}{2}}}}{(\epsilon_s^2(k) + (\Delta_s(k) - M)^2)^{\frac{1}{2}} + \frac{\Delta_s(k)\{\Delta_s(k) - M\}}{(\epsilon_s^2(k) + (\Delta_s(k) - M)^2)^{\frac{1}{2}}}}\right) d\epsilon_s(k), \end{aligned} \tag{70}$$

$$= \int_0^{\hbar\omega_F} \frac{\beta M^2}{2} \frac{\operatorname{sech}^2 \frac{\beta}{2}(\epsilon_s^2(k) + M^2)^{\frac{1}{2}} \frac{\beta}{2} \frac{1}{(\epsilon_s^2(k) + M^2)^{\frac{1}{2}}}}{(\epsilon_s^2(k) + M^2)^{\frac{1}{2}}} d\epsilon_s(k), \tag{71}$$

$$= \int_0^{\hbar\omega_F} \frac{\beta^2 M^2}{4} \frac{\operatorname{sech}^2 \frac{\beta}{2}(\epsilon_s^2(k)+M^2)^{\frac{1}{2}}}{\epsilon_s^2(k)+M^2} d\epsilon_s(k). \tag{72}$$

After some steps, Equation (72) becomes the following:

$$I_2 = -\frac{\beta M}{4} ln\left(\frac{\hbar\omega_F + M}{\hbar\omega_F - M}\right) + \int_0^{\hbar\omega_F} \frac{\beta M^2}{2} \frac{\tanh^2\left(\frac{\beta}{2}(\epsilon_s^2(k)+M^2)^{\frac{1}{2}}\right)}{(\epsilon_s^2(k)+M^2)^{\frac{1}{2}}} d\epsilon_s(k). \tag{73}$$

Now Equation (54) yields,

$$h_1 = \ln\left(1.14\frac{\hbar\omega_F}{k_B T_c}\right) - 1.052\left(\frac{M}{\pi k_B T_c}\right)^2 - \frac{\beta M}{4} ln\left(\frac{\hbar\omega_F + M}{\hbar\omega_F - M}\right) + \int_0^{\hbar\omega_F} \frac{\beta M^2}{2} \frac{\tanh^2\left(\frac{\beta}{2}(\epsilon_s^2(k)+M^2)^{\frac{1}{2}}\right)}{(\epsilon_s^2(k)+M^2)^{\frac{1}{2}}} d\epsilon_s(k). \tag{74}$$

Applying the same procedure h_2 can be written as follows:

$$h_2 = \ln\left(1.14\frac{\hbar\omega_F}{k_B T_c}\right) - 1.052\left(\frac{M}{\pi k_B T_c}\right)^2 - \frac{\beta M}{4} ln\left(\frac{\hbar\omega_F + M}{\hbar\omega_F - M}\right) - \int_0^{\hbar\omega_F} \frac{\beta M^2}{2} \frac{\tanh^2\left(\frac{\beta}{2}(\epsilon_s^2(k)+M^2)^{\frac{1}{2}}\right)}{(\epsilon_s^2(k)+M^2)^{\frac{1}{2}}} d\epsilon_s(k). \tag{75}$$

Substituting Equations (74) and (75) into Equation (51), it gives the following:

$$\frac{1}{\varphi} = \ln\left(1.14\frac{\hbar\omega_F}{k_B T_c}\right) - 1.052\left(\frac{M}{\pi k_B T_c}\right)^2 - \frac{\beta M}{4} ln\left(\frac{\hbar\omega_F + M}{\hbar\omega_F - M}\right). \tag{76}$$

For small M, one can ignore the M^2 term. Thus, Equation (76) reduces to the following:

$$\frac{1}{\varphi} = \ln\left(1.14\frac{\hbar\omega_F}{k_B T_c}\right) - \frac{\beta M}{4} ln\left(\frac{\hbar\omega_F + M}{\hbar\omega_F - M}\right), \tag{77}$$

$$= \ln\left(1.14\frac{\hbar\omega_F}{k_B T_c}\right) - \frac{M}{4k_B T_c} ln\left(\frac{\hbar\omega_F + M}{\hbar\omega_F - M}\right), \tag{78}$$

$$\exp\left(\frac{1}{\varphi}\right) = 1.14\frac{\hbar\omega_F}{k_B T_c}\exp\left(-\frac{M}{4k_B T_c} ln\left(\frac{\hbar\omega_F + M}{\hbar\omega_F - M}\right)\right), \tag{79}$$

$$T_c = 1.14\frac{\hbar\omega_F}{k_B}\exp\left(-\frac{1}{\varphi} - \frac{M}{4k_B T_c} ln\left(\frac{\hbar\omega_F + M}{\hbar\omega_F - M}\right)\right). \tag{80}$$

The expression for dependence of T_c on M in the inter band interaction becomes the following:

$$T_c = 1.14\frac{\hbar\omega_F}{k_B}\exp\left(-\frac{1}{\varphi} - \frac{M}{4k_B T_c} ln\left(\frac{\hbar\omega_F + M}{\hbar\omega_F - M}\right)\right). \tag{81}$$

Equation (81) clearly shows the dependence of the SC transition temperature on the SDW order parameter. In the pure diamagnetism region, $M = 0$, and Equation (81) becomes the following:

$$T_c = 1.14\frac{\hbar\omega_F}{k_B}\exp\left(-\frac{1}{\varphi}\right). \tag{82}$$

This is like the well-known BCS expression for the SC transition temperature (T_c). From Equation (82), the SC coupling parameter can be found as follows:

$$\frac{1}{\varphi} = \ln\left(1.14\frac{\hbar\omega_F}{k_B T_c}\right), \tag{82.1}$$

where $\hbar\omega_F = 84.2\text{meV}$, $T_c = 38\text{K}$ [21, 25, 30] and $k_B = 0.08617\text{meV/K}$. Substituting these values in Equation (82.1), we will have $\frac{1}{\varphi} = ln\left[\frac{1.14x84.2mev}{0.08617meV/Kx38K}\right] = \ln\left[\frac{95.988}{3.27446}\right] = \ln[29.314] = 3.378\,\varphi = \frac{1}{3.378} = 0.296$

For perfect diamagnetism $M = 0$ Equation (50) gives the following:

$$\frac{1}{\varphi} = \int_0^{\hbar\omega_F} \frac{\tanh\frac{\beta}{2}(\epsilon_s^2(k)+\Delta_s{}^2)^{\frac{1}{2}}}{(\epsilon_s^2(k)+\Delta_s{}^2)^{\frac{1}{2}}} d\epsilon_s(k). \tag{83}$$

After some steps, Equation (83) becomes the following:

$$\frac{1}{\varphi} = \ln\left(1.14\frac{\hbar\omega_F}{k_B}\right) - 1.052\left(\frac{\Delta_s)}{\pi k_B T_c}\right)^2. \tag{84}$$

From the BCS theory,

$$k_B T_c = 1.14\hbar\omega_F\exp\left(-\frac{1}{\varphi}\right), \tag{85}$$

$$\frac{1}{\varphi} = \ln\left(1.14\frac{\hbar\omega_F}{k_B T_c}\right), \tag{86}$$

$$\ln\left(1.14\frac{\hbar\omega_F}{k_B T_c}\right) = \ln\left(1.14\frac{\hbar\omega_F}{k_B T_c}\right) - 1.052\left(\frac{\Delta_s}{\pi k_B T_c}\right)^2, \tag{87}$$

$$\ln\left(\frac{T}{T_c}\right) = -1.052\left(\frac{\Delta_s}{\pi k_B T_c}\right)^2. \tag{88}$$

Using logarithmic series

$$\ln(1 \pm x) = \pm x - \frac{1}{2}x^2 \pm \frac{1}{3}x^3 -, \tag{89}$$

$$\ln\left(1 - \left(1 - \frac{T}{T_c}\right)\right) = -\left(1 - \frac{T}{T_c}\right) - \frac{1}{2}\left(1 - \frac{T}{T_c}\right)^2 - \frac{1}{3}\left(1 - \frac{T}{T_c}\right)^3 - . \tag{90}$$

Ignoring the high-order terms, it reduces to the following:

$$\ln\left(1 - \left(1 - \frac{T}{T_c}\right)\right) \approx -\left(1 - \frac{T}{T_c}\right), \tag{91}$$

$$-\left(1 - \frac{T}{T_c}\right) = -1.052\left(\frac{\Delta_s(k)}{\pi k_B T_c}\right)^2, \tag{92}$$

$$\Delta_s(T) = 3.063 k_\beta T_c\left(1 - \frac{T}{T_c}\right)^{\frac{1}{2}}. \tag{93}$$

2.4. Magnetic Order Parameter (M). Using the Bogoliubov transformation, we defined for SDW state in Equation (23); we are now able to calculate the expectation value of the operators in Equation (22) with SC state, the SDW gap equation or SDW order parameter M is given by the following:

$$M = \frac{U}{\beta}\sum_k \left\langle \hat{a}^{\dagger}_{k\uparrow}, \hat{b}_{(k+p)\downarrow} \right\rangle. \tag{94}$$

Applying the same procedure as for the pure SDW region, Equation (94) is simplified.

$$M = \sum_k U \left[\frac{-(\Delta_s(k) + M(k))}{2E(k)}\tanh\beta\left[\frac{E_A(k)}{2}\right] + \frac{(\Delta_s(k) - M(k))}{2E(k)}\tanh\beta\left[\frac{E_A(k)}{2}\right]\right], \tag{95}$$

where

$$E(k) = \sqrt{\epsilon_s^2(k) + (\Delta_s(k) + M(k))^2}, \tag{96}$$

$$\begin{aligned} E_A(k) &= \sqrt{\epsilon_s^2(k) + (\Delta_s(k) + M(k))^2} \\ E_B(k) &= \sqrt{\epsilon_s^2(k) + (\Delta_s(k) - M(k))^2} \end{aligned}. \tag{97}$$

Equation (95) can be simplified as follows:

$$M = \frac{U}{4}\sum_{j=1} \frac{(-1)^j \Delta_j(k)\tanh\frac{\beta}{2}\sqrt{\epsilon_s^2(k) + \Delta_j{}^2(k)}}{\sqrt{\epsilon_s^2(k) + \Delta_j{}^2(k)}}, \tag{98}$$

where $\Delta_j = \Delta_s - (-1)^j M$, which is the effective order parameter. $E(k) = \sqrt{\epsilon_s^2(k) + \Delta_j{}^2(k)}$.

Changing the summation to integration in the region $-\hbar\omega_F < \epsilon_s(k) < \hbar\omega_F$ and by introducing the density of state at the Fermi level is $N(0)$ that is as follows:

$$\sum_k \approx \int_{-\hbar\omega_F}^{\hbar\omega_F} N(0) d\epsilon_s(k). \tag{99}$$

Inserting Equation (99) into Equation (98), we get the following:

$$M = \frac{U}{4}\int_{-\hbar\omega_F}^{\hbar\omega_F} N(0) \frac{(-1)^j \Delta_j(k)\tanh\frac{\beta}{2}\sqrt{\epsilon_s^2(k) + \Delta_j{}^2(k)}}{\sqrt{\epsilon_s^2(k) + \Delta_j{}^2(k)}} d\epsilon_s(k), \tag{100}$$

$$= \frac{UN(0)}{4}\int_{-\hbar\omega_F}^{\hbar\omega_F} \frac{(-1)^j \Delta_j(k)\tanh\frac{\beta}{2}\sqrt{\epsilon_s^2(k) + \Delta_j{}^2(k)}}{\sqrt{\epsilon_s^2(k) + \Delta_j{}^2(k)}} d\epsilon_s(k). \tag{101}$$

Say $\psi = UN(0)$, which is called the magnetic coupling parameter.

$$M = \frac{(-1)^j \psi \Delta_j}{4}\int_{-\hbar\omega_F}^{\hbar\omega_F} \frac{\tanh\frac{\beta}{2}\sqrt{\epsilon_s^2(k) + \Delta_j{}^2(k)}}{\sqrt{\epsilon_s^2(k) + \Delta_j{}^2(k)}} d\epsilon_s(k), \tag{102}$$

$$\frac{4}{\psi} = \frac{(-1)^j \Delta_j}{M}\int_{-\hbar\omega_F}^{\hbar\omega_F} \frac{\tanh\frac{\beta}{2}\sqrt{\epsilon_s^2(k) + \Delta_j{}^2(k)}}{\sqrt{\epsilon_s^2(k) + \Delta_j{}^2(k)}} d\epsilon_s(k), \tag{103}$$

$$\frac{2}{\psi} = \frac{(-1)^j \Delta_j}{M}\int_{0}^{\hbar\omega_F} \frac{\tanh\frac{\beta}{2}\sqrt{\epsilon_s^2(k) + \Delta_j{}^2(k)}}{\sqrt{\epsilon_s^2(k) + \Delta_j{}^2(k)}} d\epsilon_s(k), \tag{104}$$

$$\frac{2}{\psi} = \frac{-(\Delta_s + M)}{M}\int_{0}^{\hbar\omega_F} \frac{\tanh\frac{\beta}{2}\sqrt{\epsilon_s^2(k) + (\Delta_s + M)^2(k)}}{\sqrt{\epsilon_s^2(k) + (\Delta_s + M)^2(k)}} d\epsilon_s(k) - \frac{(\Delta_s - M)}{M}\int_{0}^{\hbar\omega_F} \frac{\tanh\frac{\beta}{2}\sqrt{\epsilon_s^2(k) + (\Delta_s - M)^2(k)}}{\sqrt{\epsilon_s^2(k) + (\Delta_s - M)^2(k)}} d\epsilon_s(k), \tag{105}$$

$$\frac{2}{\psi} = -\left(1+\frac{\Delta_s}{M}\right)\int_0^{\hbar\omega_F}\frac{\tanh\frac{\beta}{2}\sqrt{\epsilon_s^2(k)+(\Delta_s+M)^2(k)}}{\sqrt{\epsilon_s^2(k)+(\Delta_s+M)^2(k)}}d\epsilon_s(k) - \left(1-\frac{\Delta_s}{M}\right)\int_0^{\hbar\omega_F}\frac{\tanh\frac{\beta}{2}\sqrt{\epsilon_s^2(k)+(\Delta_s-M)^2(k)}}{\sqrt{\epsilon_s^2(k)+(\Delta_s-M)^2(k)}}d\epsilon_s(k). \tag{106}$$

After some steps, one gets,

$$\frac{1}{\psi} = \ln\left(1.14\frac{\hbar\omega_F}{k_BT_M}\right) - 1.052\left(\frac{M}{\pi k_BT_M}\right)^2 + \frac{\beta M}{4}ln\left(\frac{\hbar\omega_F+M}{\hbar\omega_F-M}\right). \tag{107}$$

For small values of M, we ignore M^2 term. Thus, Equation (107) reduces to the following:

$$\frac{1}{\psi} = \ln\left(1.14\frac{\hbar\omega_F}{k_BT_M}\right) + \frac{\beta M}{4}ln\left(\frac{\hbar\omega_F+M}{\hbar\omega_F-M}\right), \tag{108}$$

$$\frac{1}{\psi} = \ln\left(1.14\frac{\hbar\omega_F}{k_BT_M}\right) + \frac{M}{4k_BT_M}ln\left(\frac{\hbar\omega_F+M}{\hbar\omega_F-M}\right), \tag{109}$$

$$T_M = 1.14\frac{\hbar\omega_F}{k_B}\exp\left(-\frac{1}{\psi}+\frac{M}{4k_BT_M}ln\left(\frac{\hbar\omega_F+M}{\hbar\omega_F-M}\right)\right), \tag{110}$$

where ψ is the SDW coupling parameter. Equation (110) shows that the SDW order parameter increases as the SDW transition temperature increases. For $M = 0$, Equation (110) is simplified to the following:

$$T_M = 1.14\frac{\hbar\omega_F}{k_B}\exp\left(-\frac{1}{\psi}\right), \tag{110.1}$$

where $\hbar\omega_F = 84.2$mev, $T_M = 140$K [21, 22, 36] and $k_B = 0.08617$meV/K. Substituting these values in Equation (110.1), we will have $\frac{1}{\psi} = ln\left[\frac{1.14x84.2mev}{0.08617meV/Kx140K}\right] = \ln\left[\frac{95.988}{12.0638}\right] = \ln[7.9567] = 2.0740\,\psi = \frac{1}{2.0740} = 0.4822$.

For pure magnetic region $\Delta_s = 0$ and Equation (106) becomes the following:

$$\frac{1}{\psi} = -\int_0^{\hbar\omega_F}\frac{\tanh\frac{\beta}{2}\sqrt{\epsilon_s^2(k)+M^2(k)}}{\sqrt{\epsilon_s^2(k)+M^2(k)}}d\epsilon_s(k). \tag{111}$$

Let say $\gamma^2 = \beta^2(\epsilon_s^2(k)+\Delta_j{}^2(k))$ and $\sum_{-\infty}^{\infty}\frac{1}{((2n+1)\pi)^2+\gamma^2} = \frac{\tanh\frac{\gamma}{2}}{2\gamma}$

$$\frac{1}{\psi} = -\int_0^{\hbar\omega_F}\frac{2\beta\tanh\frac{\gamma}{2}}{2\gamma}d\epsilon_s(k), \tag{112}$$

$$= -2\beta\int_0^{\hbar\omega_F}\sum_{-\infty}^{\infty}\frac{1}{((2n+1)\pi)^2+\gamma^2}d\epsilon_s(k), \tag{113}$$

$$= -\frac{\beta}{2}\int_0^{\hbar\omega_F}\sum_{-\infty}^{\infty}\frac{1}{\omega_n^2+\epsilon_s(k)+M^2(k}d\epsilon_s(k). \tag{114}$$

From Laplacian transform with the Matsuber relation result, we can write the equation as follows:

$$\frac{\beta}{2}\int_0^{\hbar\omega_F}\sum_{-\infty}^{\infty}\frac{1}{\omega_n^2+\epsilon_s^2(k)+M^2(k)}d\epsilon_s(k) = \frac{\beta}{2}\int_0^{\hbar\omega_F}\sum_{-\infty}^{\infty}\frac{1}{\omega_n^2+\epsilon_s^2(k)}d\epsilon_s(k) - \frac{\beta M^2}{2}\int_0^{\hbar\omega_F}\sum_{-\infty}^{\infty}\frac{1}{\omega_n^2+\epsilon_s^2(k)}d\epsilon_s(k), \tag{115}$$

$$= 2\beta\int_0^{\hbar\omega_F}\sum_{-\infty}^{\infty}\frac{1}{((2n+1)\pi)^2+\beta^2\epsilon_s^2(k)}d\epsilon_s(k) - M^2\int_0^{\hbar\omega_F}\frac{2}{\beta}\sum_{-\infty}^{\infty}\frac{1}{\left(\frac{(2n+1)\pi}{\beta}\right)^2+\epsilon_s^2(k)}d\epsilon_s(k), \tag{116}$$

$$= \int_0^{\hbar\omega_F}\frac{\tanh\beta\frac{\epsilon_s(k)}{2}}{\epsilon_s(k)}d\epsilon_s(k) - 2M^2\int_0^{\hbar\omega_F}\frac{2}{\beta}\sum_0^{\infty}\frac{1}{(2n+1)^2\left(\frac{\pi}{\beta}\right)^2+\epsilon_s^2(k)}d\epsilon_s(k). \tag{117}$$

Now let us apply the following equality:

$$\sum_0^{\infty}\frac{1}{(f^2+\epsilon_s^2(k))^2}d\epsilon_s(k) = 2\sum_0^{\infty}\frac{1}{f^4(1+z^2)^2}d\epsilon_s(k), \tag{118}$$

where $f^2 = (2n+1)^2\left(\frac{\pi}{\beta}\right)^2$ and $z^2 = \frac{\epsilon_s^2(k)}{f^2}$

$$\frac{\beta}{2}\int_0^{\hbar\omega_F}\sum_{-\infty}^{\infty}\frac{1}{\omega_n^2+\epsilon_s^2(k)+M^2}d\epsilon_s(k) = \int_0^{\hbar\omega_F}\frac{\tanh\beta\frac{\epsilon_s(k)}{2}}{\epsilon_s(k)}d\epsilon_s(k) - \int_0^{\hbar\omega_F}\frac{4}{\beta}\sum_0^{\infty}\frac{M^2}{f^4(1+z^2)^2}d\epsilon_s(k). \tag{119}$$

From the above equality relations $z = \beta\frac{\epsilon_s(k)}{2}$ and $dz = \beta\frac{d\epsilon_s(k)}{2}$

$$\frac{\beta}{2}\int_0^{\hbar\omega_F}\sum_{-\infty}^{\infty}\frac{1}{\omega_n^2+\epsilon_s^2(k)+M^2}d\epsilon_s(k) = \int_0^{\frac{\beta}{2}\hbar\omega_F}\frac{\tanh z}{z}dz - \int_0^{\infty}\frac{4}{\beta}\sum_0^{\infty}\frac{M^2}{f^3(1+z^2)^2}dz, \tag{120}$$

$$= \ln\left(\frac{\beta}{2}\hbar\omega_F\right)\tanh\left(\frac{\beta}{2}\hbar\omega_F\right) - \int_0^{\frac{\beta}{2}\hbar\omega_F}\frac{\ln z}{\cosh^2 z}dz - \frac{4}{\beta}M^2\sum_0^{\infty}\frac{1}{f^3}\int_0^{\infty}\frac{1}{(1+z^2)^2}dz, \tag{121}$$

$$= \ln\left(\frac{\beta}{2}\hbar\omega_F\right)\tanh\left(\frac{\beta}{2}\hbar\omega_F\right) - \ln\left(\frac{\pi}{4\gamma}\right) - \frac{4\beta^2M^2}{\pi^3}\sum_0^\infty \frac{1}{(2n+1)^3}\int_0^\infty \frac{1}{(1+z^2)^2}dz, \tag{122}$$

$$= \ln\left(\frac{\beta}{2}\hbar\omega_F\right)\tanh\left(\frac{\beta}{2}\hbar\omega_F\right) - \ln\left(\frac{\pi}{4\gamma}\right) - \frac{4\beta^2M^2}{\pi^3}\frac{7}{8}\xi(3)\frac{\pi}{4}. \tag{123}$$

For low-temperature $\tanh\left(\frac{\beta}{2}\hbar\omega_F\right) \longrightarrow 1$ and γ denotes the Euler's constant and its value is given by $\gamma = 1.78$. $\int_0^\infty \frac{1}{1+z^2}dz = \frac{\pi}{4}$ and $\sum_0^\infty \frac{1}{(2n+1)^p} = (1-2^{-p})\xi(p)$ this means $\xi(3) = 1.202$. so Equation (123) can be written as follows:

$$\frac{\beta}{2}\int_0^{\hbar\omega_F}\sum_{-\infty}^{\infty}\frac{1}{\omega_n^2+\epsilon_s^2(k)+M^2)}d\epsilon_s(k) = \ln\left(\frac{\beta}{2}\hbar\omega_F\right) - \ln\left(\frac{\pi}{4\gamma}\right) - \frac{4\beta^2\Delta_j{}^2(k)}{\pi^3}\frac{7}{8}(1.202)\frac{\pi}{4}, \tag{124}$$

$$= \ln\left(1.14\frac{\hbar\omega_F}{k_BT}\right) - M^2\left(\frac{1}{\pi k_BT}\right)^2 1.052. \tag{125}$$

Therefore, it gives the following:

$$-\frac{1}{\psi} = \ln\left(1.14\frac{\hbar\omega_F}{k_BT}\right) - M^2\left(\frac{1}{\pi k_BT}\right)^2 1.052. \tag{126}$$

For a very small value of M, M^2 goes to zero and $T \longrightarrow T_M$. The magnetic coupling parameter becomes as follows:

$$-\frac{1}{\psi_j} = \ln\left(1.14\frac{\hbar\omega_F}{k_BT_M}\right). \tag{127}$$

Substituting Equation (127) into Equation (126), we get the following:

$$\ln\left(1-\left(1-\frac{T}{T_M}\right)\right) = -M^2(k)\left(\frac{1}{\pi k_BT_M}\right)^2 1.052. \tag{128}$$

After some steps, we get the following:

$$M = \frac{\pi k_BT_M}{1.052}\left(1-\frac{T}{T_M}\right)^{\frac{1}{2}}. \tag{129}$$

The expression for the temperature dependence of SDW in the temperature range of $0 \le T \le 140K$ [36] becomes the following:

$$M(T) = 3.063k_\beta T_M\left(1-\frac{T}{T_M}\right)^{\frac{1}{2}}. \tag{130}$$

This equation tells that if the temperature increases, the SDW order parameter decreases.

3. Result and Discussion

In this chapter, the effect of temperature (T) on the SC order parameter (Δ_s) and SDW order parameter (M) on the SC transition temperature (T_c) and on SDW transition temperature(T_M). It also describes the analysis we made for the conceptual analysis of the interplay of superconductivity and SDW in a two-band model for $Ba_{1-x}K_xFe_2As_2$. Using a two-band model Hamiltonian and using Bogoliubov transformation formalism, one obtained the mathematical expressions for the SC transition temperature (T_c), the SDW transition temperature(T_M), the SC order parameter(Δ_s) and the SDW order parameter (M).

From Equations (82) and (93) and using the MATLAB script, we plot the phase diagram Δ_S (meV) versus T (K) as Figure 1(a) illustrates this. Based on Equation (130), the phase diagram showing how the magnetic order parameter (M) depends on the temperature in the pure magnetic region shown in Figure 1(b) was plotted.

As seen in Figure 1(a), when the temperature increases, the SC order parameter decreases and gets lost as the temperature is equal to the critical temperature. The maximum value of SC order parameter, $\Delta_S = 10.01$meV, occurs at $T = 0$ and it vanishes at the SC transition temperature $T_c = 38$ K. As Figure 1(b) shows, magnetism decreases as the temperature increases and becomes lost at the SDW transition temperature $T_M = 140$ K. The maximum value of the SDW order parameter, $M = 36.9514$ meV, occurs at $T = 0$. This finding is also in agreement with experimental observations [21, 23, 25, 30, 37].

Based on Equation (81), we plotted the phase diagrams of T_c versus M. As can be observed in Figure 2(a), the SC transition temperature is suppressed as the value of the the SDW order parameter increases for $Ba_{1-x}K_xFe_2As_2$. From this figure, one can observe that the SDW order parameter suppresses superconductivity and increases the magnetic nature of the system.

Using Equation (110), one also plotted the phase diagram of the transition temperature (T_M) versus SDW order parameter of SDW (M) (Figure 2(b)). As can be observed from the figure, T_M increases with increasing SDW order parameter of the $Ba_{1-x}K_xFe_2As_2$ superconductor.

Finally, by merging Figures 2(a) and 2(b), one depicted a region where both superconductivity and SDW coexist, as shown in Figure 3. This figure shows the possible interplay of superconductivity and SDW for $Ba_{1-x}K_xFe_2As_2$. As indicated in this figure, this finding is in agreement with experimental observations [21, 25, 30]. This figure also depicts there are regions that show SC state and antiferromagnetic state segregates, which indicates that there are regions where magnetic and SC phases are not mixed.

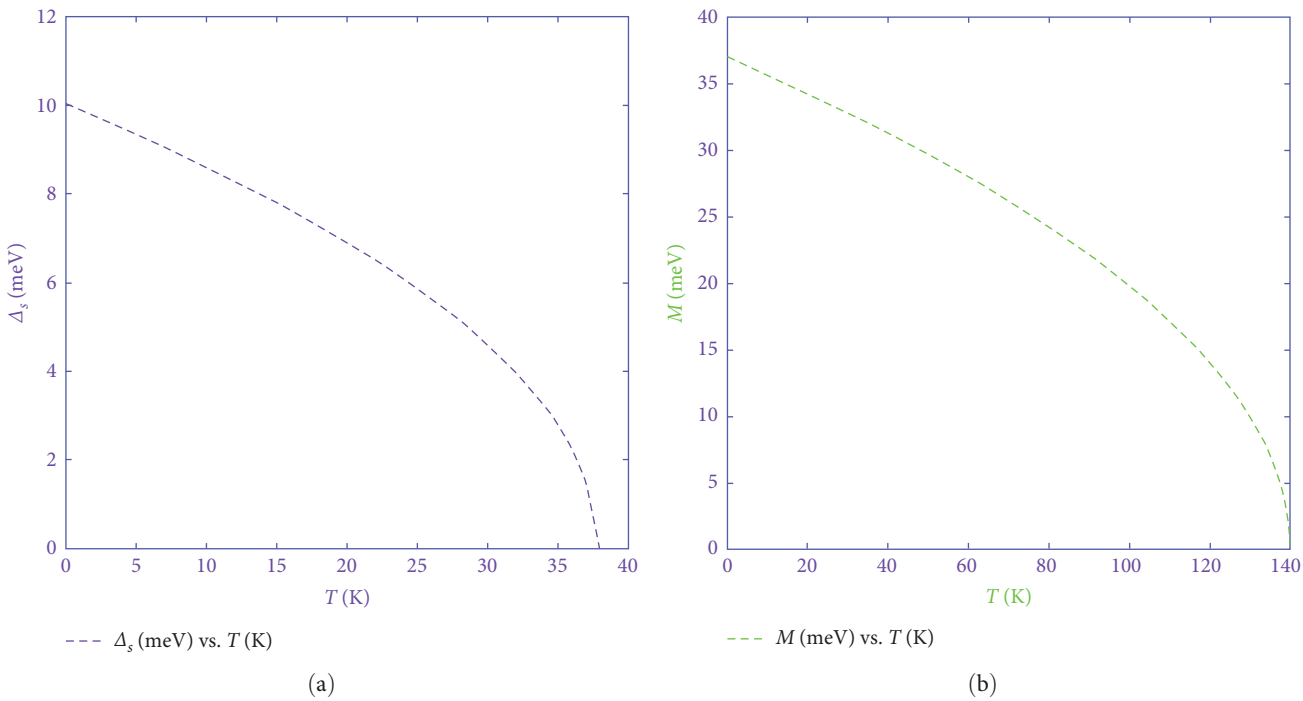

FIGURE 1: The phase diagram of superconducting order parameter vs. temperature for our compound $Ba_{1-x}K_xFe_2As_2$ superconductor (a) and the phase diagram of SDW order parameter (M) vs. temperature in the pure magnetic region of the $Ba_{1-x}K_xFe_2As_2$ superconductor (b).

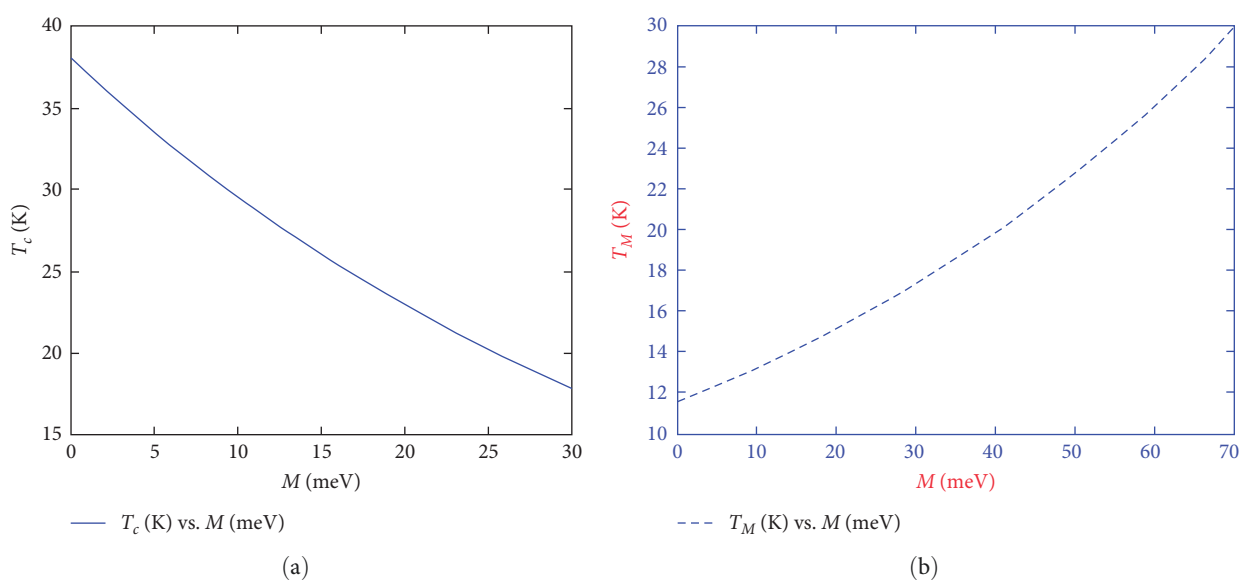

FIGURE 2: The phase diagram superconducting transition temperature (T_c) versus SDW order parameter(M) for $Ba_{1-x}K_xFe_2As_2$ superconductor (a) and the phase diagram of SDW transition temperature(T_M)versus SDW order parameter(M) of the $Ba_{1-x}K_xFe_2As_2$ superconductor (b).

4. Conclusions

In this work, the possible coexistence of superconductivity and magnetism has been studied in the two-band model for the iron-based superconductor $Ba_{1-x}K_xFe_2As_2$. The superconductivity order parameter is weakened when the temperature increases and gets lost at the SC critical temperature. The SC transition temperature is weakened as the magnitude of the SDW order parameter increases. The SDW transition temperature increases with increasing SDW order parameter for $Ba_{1-x}K_xFe_2As_2$. This finding also proofs the dependence of the SDW order parameter on the temperature in the pure magnetic region of the iron-based superconductor $Ba_{1-x}K_xFe_2As_2$. The SDW order parameters is weakened when the temperature

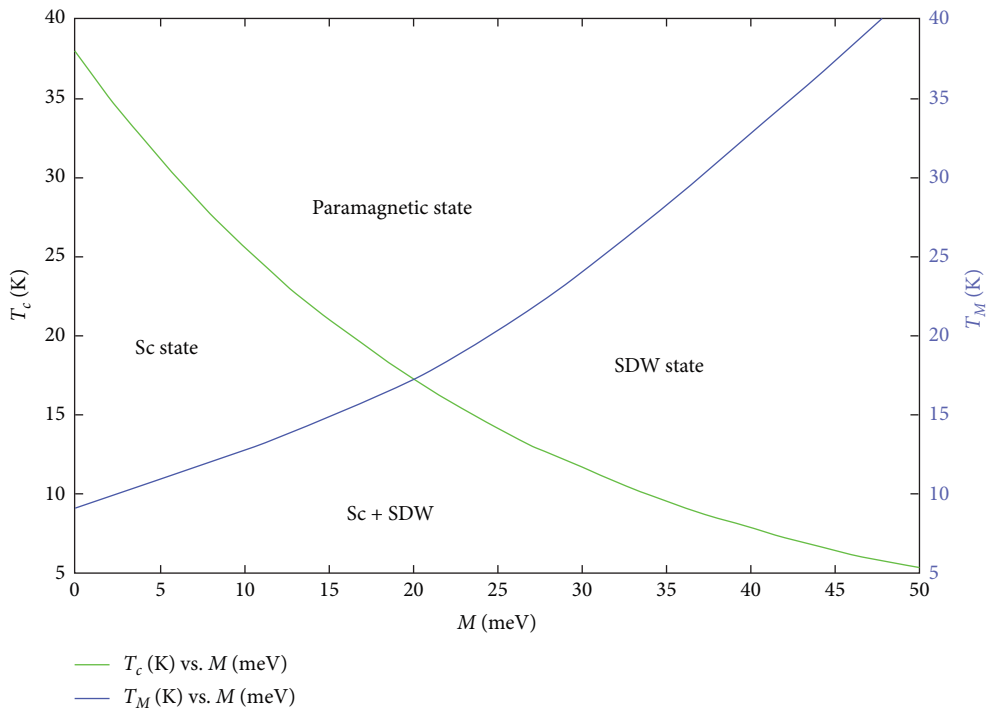

FIGURE 3: Phase diagram of the superconducting critical temperature and magnetic transition temperature vs. the SDW order parameter of the $Ba_{1-x}K_xFe_2As_2$ superconductor.

increases and vanishes at the SDW transition temperature. We have depicted the possible interplay of superconductivity and magnetism of the $Ba_{1-x}K_xFe_2As_2$ superconductor. The possible interplay of superconductivity and magnetism in $Ba_{1-x}K_xFe_2As_2$ initiates further study in the field of condensed matter physics for further studies. The results obtained in this article work are in agreement with previous studies [25, 30] that the coexistence implies that there is a weak exchange coupling between the itinerant SC electrons and the localized ordered spins in the $Ba_{1-x}K_xFe_2As_2$ superconductor.

Data Availability

The data used to support the findings of this study are included in the article.

Ethical Approval

The conducted research is not related to either human or animal use.

Conflicts of Interest

The authors declare that they have no conflicts of interest.

Authors' Contributions

All authors contributed equally to this study. That is, they analyzed the data, drafted and edited the manuscript, and read and approved the final manuscript.

References

[1] R. M. Fernandes, A. I. Coldea, H. Ding, I. R. Fisher, P. J. Hirschfeld, and G. Kotliar, "Iron pnictides and chalcogenides: a new paradigm for superconductivity," *Nature*, vol. 601, pp. 35–44, 2022.

[2] A. Kreisel, P. J. Hirschfeld, and B. M. Andersen, "On the remarkable superconductivity of FeSe and its close cousins," *Symmetry*, vol. 12, no. 9, Article ID 1402, 2020.

[3] B. Roter, N. Ninkovic, and S. V. Dordevic, "Clustering superconductors using unsupervised machine learning," *Physica C: Superconductivity and its Applications*, vol. 598, Article ID 1354078, 2022.

[4] T. K. Kim, K. S. Pervakov, D. V. Evtushinsky et al., "Electronic structure and coexistence of superconductivity with magnetism in Rb Eu Fe_4 As_4," *Physical Review*, vol. 103, no. 17, Article ID 174517, 2021.

[5] A. B. Yu, Z. Huang, C. Zhang et al., "Superconducting anisotropy and vortex pinning in $CaKFe_4As_4$ and KCa_2-$Fe_4As_4F_2$," *Chinese Physics B*, vol. 30, no. 2, Article ID 027401, 2021.

[6] H. Hosono, A. Yamamoto, H. Hiramatsu, and Y. Ma, "Recent advances in iron-based superconductors toward applications," *Materialstoday*, vol. 21, no. 3, pp. 278–302, 2018.

[7] G. Bioletti, *The Interplay of Pressure and Doping Effects on $BaFe_2As_2$ Superconductors*, Open Access Te Herenga Waka-Victoria University of Wellington), 2022.

[8] S. K. Shrivastava and G. Kumar, "High-tc superconductivity in iron-based pnictides and chalcogenides," *International Journal of Emerging Technologies and Innovative Research*, vol. 6, no. 5, pp. 417–426, 2019.

[9] M. Hesani, K. Rahimi, and A. Yazdani, "Charge-doping-induced variation of the superconducting $BaFe_2As_2$ electronic structure and the emerging physical effects a

DFT$^+$ DMFT study," *Journal of Materials*, vol. 56, pp. 14157–14169, 2021.

[10] G. Liu, Z.-B. Huang, and Y.-J. Wang, "Quantum Monte Carlo study of the S_4 symmetric microscopic model for iron-based superconductors," *The European Physical Journal B*, vol. 92, Article ID 42, 2019.

[11] R. Yu, H. Hu, E. M. Nica, J.-X. Zhu, and Q. Si, "Orbital selectivity in electron correlations and superconducting pairing of iron-based superconductors," *Frontiers in Physics*, vol. 9, Article ID 578347, 2021.

[12] S. Qin, C. Fang, F.-C. Zhang, and J. Hu, "Topological superconductivity in an extended *s*-wave superconductor and its implication to iron-based superconductors," *Physical Review X*, vol. 12, no. 1, Article ID 011030, 2022.

[13] G. Biswal and K. L. Mohanta, "A recent review on iron-based superconductor," *Materials Today: Proceeding*, vol. 35, pp. 207–215, 2021.

[14] S. Tokuta and A. Yamamoto, "Enhanced upper critical field in Co-doped Ba122 superconductors by lattice defect," *APL Materials*, vol. 7, no. 11, Article ID 111107, 2019.

[15] G. Ghigo, M. Fracasso, R. Gerbaldo et al., "High-frequency ac susceptibility of iron-based superconductors," *Materials*, vol. 15, no. 3, Article ID 1079, 2022.

[16] F. Waßer, J. T. Park, S. Aswartham et al., "Strong spin resonance mode associated with suppression of soft magnetic ordering in hole-doped $Ba_{1-x}Na_xFe_2As_2$," *NPJ Quantum Materials*, vol. 4, Article ID 59, 2019.

[17] G. M. Bogale and D. A. Shiferaw, "High entropy materials-microstructures and properties," in *Iron-Based Superconductors*, pp. 1–19, Intech Open, 2022.

[18] G. Bioletti, G. V. M. Williams, M. A. Susner, T. J. Haugan, D. M. Uhrig, and S. V. Chong, "The effect of pressure and doping on the critical current density in nickel doped $BaFe_2As_2$," *Superconductor Science and Technology*, vol. 32, no. 6, Article ID 064001, 2019.

[19] K. S. Pervakov and V. A. Vlasenko, "Synthesis of electron-and hole-doped bulk $BaFe_2As_2$ superconductors by mechanical alloying," *Ceramics International*, vol. 46, no. 7, pp. 8625–8630, 2020.

[20] K. R. Joshi, N. M. Nusran, M. A. Tanatar et al., "Quantum phase transition inside the superconducting dome of $Ba(Fe_{1-x}Co_x)_2As_2$ from diamond-based optical magnetometry," *New Journal of Physics*, vol. 22, Article ID 053037, 2020.

[21] D. Swain, S. Ghosh, K. Bera et al., "Possible raman signature of broken symmetry states near the quantum critical point in P doped $BaFe_2As_2$: experiment and theory," *Physica C Superconductivity and its Applications*, vol. 606, Article ID 1354211, 2023.

[22] Z. Xin, Y. Wang, C. Cai et al., "Revealing the intrinsic superconducting gap anisotropy in surface-neutralized $BaFe_2(As_{0.7}P_{0.3})_2$," *Communications Physics*, vol. 4, Article ID 31, 2021.

[23] M. Bonura, H. Huang, C. Yao, Y. Ma, and C. Senatore, "Current transport, magnetic and elemental properties of densified Ag-sheathed $Ba_{1-x}K_xFe_2As_2$ tapes," *Superconductor Science and Technology*, vol. 33, no. 9, Article ID 095008, 2020.

[24] Z. W. Dlamini, A. Srinivasan, Y. Ma, and V. V. Srinivasu, "Electron spin resonance in the superconducting state of $Ba_{0.6}K_{0.4}Fe_2As_2$," *AIP Conference Proceedings*, vol. 1953, no. 1, Article ID 120079, 2018.

[25] M. D. Watson, P. Dudin, L. C. Rhodes et al., "Probing the reconstructed Fermi surface of antiferromagnetic $BaFe_2As_2$ in one domain," *NPJ Quantum Materials*, vol. 4, Article ID 36, 2019.

[26] G. Romain, K. Kota, P. Massat et al., "Terahertz pulse-driven collective mode in the nematic superconducting state of $Ba_{1-x}K_xFe_2As_2$," *NPJ Quantum Materials*, vol. 7, Article ID 4, 2022.

[27] T. Zhou, "Characteristic frequency of the orbital fluctuation in the unconventional iron-based superconductor $BaFe_2As_2$: a TDDFT investigation of the electron pairing mechanism," 2019.

[28] K. V. Mitsen and O. M. Ivanenko, "Cluster structure of superconducting phase and the nature of peaks in the doping dependences of the London penetration depth in iron pnictides," *Results in Physics*, vol. 32, Article ID 105156, 2022.

[29] T. Böhm, F. Kretzschmar, A. Baum et al., "Microscopic origin of cooper pairing in the iron-based superconductor $Ba_{1-x}K_xFe_2As_2$," *NPJ Quantum Materials*, vol. 3, Article ID 48, 2018.

[30] D. Johrendt and R. Pöttgen, "Superconductivity, magnetism and crystal chemistry of $Ba_{1-x}K_xFe_2As_2$," *Physica C: Superconductivity*, vol. 469, no. 9–12, pp. 332–339, 2009.

[31] T. Lissanu, "Parameterization of high temperature superconductivity in two band model for the iron based superconductor $Ba_{1-x}Na_xFe_2As_2$ (Doctoral dissertation)," 2022.

[32] T. Kidanemariam, G. Kahsay, and A. Mebrahtu, "Theoretical investigation of the coexistence of superconductivity and spin density wave (SDW) in two-band model for the iron-based superconductor $BaFe_2(As_{1-x}P_x)_2$," *The European Physical Journal B*, vol. 92, Article ID 39, 2019.

[33] R. Mohapatra and G. C. Rout, "Spin density wave interaction in two band model for the iron-based superconductors," *International Journal of Scientific & Engineering Research*, vol. 5, no. 3, pp. 2229–5518, 2014.

[34] R. Mohapatra and G. Rout, "Co-existence of spin density wave and Jahn–Teller distortion in iron oxypinctide superconductors: a two band tight-binding model approach," *Orissa Journal of Physics*, vol. 26, no. 2, pp. 97–105, 2019.

[35] G. Xu, X. Zhang, C. Yao et al., "Effects of different directional rolling on the fabrication of 7-filament $Ba_{1-x}K_xFe_2As_2$ tapes," *Physica C: Superconductivity and its Applications*, vol. 561, pp. 30–34, 2019.

[36] M. H. Christensen, B. M. Andersen, and P. Kotetes, "Unravelling incommensurate magnetism and its emergence in iron-based superconductors," *Physical Review X*, vol. 8, no. 4, Article ID 041022, 2018.

[37] G. Ghigo, D. Torsello, R. Gerbaldo, L. Gozzelino, F. Laviano, and T. Tamegai, "Effects of heavy-ion irradiation on the microwave surface impedance of $(Ba_{1-x}K_x)Fe_2As_2$ single crystals," *Superconductor Science and Technology*, vol. 31, no. 3, Article ID 034006, 2018.

[38] A. Park, S. Pyon, K. Ohara et al., "Field-driven transition in the $Ba_{1-x}K_xFe_2As_2$ superconductor with splayed columnar," *Physical Review B*, vol. 97, no. 6, Article ID 064516, 2018.

[39] C. C. Homes, Y. M. Dai, A. Akrap, S. L. Bud'ko, and P. C. Canfield, "Vibrational anomalies in AFe_2As_2 (A = Ca, Sr, and Ba) single crystals," *Physical Review B*, vol. 98, no. 3, Article ID 035103, 2018.

[40] J.-H. Kang, J.-W. Kim, P. J. Ryan et al., "Superconductivity in undoped $BaFe_2As_2$ by tetrahedral geometry design," *Proceedings of the National Academy of Sciences*, vol. 117, no. 35, pp. 21170–21174, 2020.